STRATIGRAPHIC VARIATION IN GRAIN SURFACE CHEMISTRY WITHIN APOLLO CORE SAMPLE 73002 USING X-RAY PHOTOELECTRON SPECTROSCOPY. C. A. Dukes[1], K.B. Stelmach[1], A. K. Woodson[1], L. Ziamanesh[1], J. Oraegbu[1], R. V. Morris[2], L. P. Keller[2], R. Christoffersen[3], C. K. Shearer[4], and the ANGSA Science Team[5]. [1]University of Virginia, Charlottesville, VA 22902 (cdukes@virginia.edu), [2]NASA JSC, Houston, TX, [3]Jacobs, NASA JSC, Houston, TX, , [4]University of New Mexico, Albuquerque, NM, [5]ANGSA Science Team list at https://www. lpi.usra.edu/ ANGSA /teams/. (cshearer@unm.edu).

Introduction: Half-a-century after the Apollo 11 manned-landing on the lunar surface, NASA released a number of previously unexamined core samples for analysis by new/improved scientific techniques. This pristine regolith includes landslide material collected near Station 3 within the Taurus-Littrow Valley on the southeastern edge of Mare Serenitatis [1-2]. Double-drive tube samples from Apollo 17: 73002 (upper ~22 cm) and the 73001 (below ~22 cm) are part of the released samples, where 73001 has been stored since 1972 in a Core-Sample Vacuum Container (CSVC) to better retain lunar volatile species (H_2O, Na, K, etc.). Sample 73001 has remained sealed since lunar acquisition. Native stratigraphy of the collected material remains preserved in the tubes, allowing analyses of grain composition, volatile content, and space-weathering products to be evaluated as a function of depth.

Space weathering by solar-wind ions and meteoritic bombardment influences the composition, chemistry, and microstructure of lunar grain rims (~100nm) [e.g. 3]. These rims, typically distinct from the bulk grain in mineralogy and morphology, develop from (1) ion impact which drives compositional change by sputtering, radiation-enhanced diffusion, implantation, radiolysis and radiosynthesis; (2) deposition of meteoritic impact melt; or (3) a convolution of the two processes. Vitrification and comminution by meteoritic impact also occurs, but typically involves the entire grain. In grains of diameter < 0.2 µm or small surface fragments ("dust"), the entire grain may exhibit signs of weathering. The importance of understanding the evolution of the grain rims and the composition of the outermost monolayers cannot be overstated; this is the portion of the lunar material that interfaces with the space environment, influencing the lunar exosphere. Additionally, rim composition provides details about lunar geochemistry, such as pyroclastic or impact events.

Experiment: "Pass 2" of regolith material from Apollo Core sample 73002 was dissected in 5 mm intervals and subsequently dry-sieved to < 1 mm size fractions within a N_2-purged lunar sample cabinet at Johnson Space Center. An allocation of 1-2 mg per interval for 15 intervals over the 18 mm closest to the surface was provided to UVa for XPS analysis from the JSC Allocation Team general allotment (~235 mg), which was correlated to additional analyses (e.g. Mossbauer maturity indices [4], Vis-NIR reflectance [4, 5], electron microscopy cosmic-ray track analysis [6]).

Lunar samples were transported in aluminum containers with PTFE caps in N_2. Because grains were typically only 10 –200 um and few in number, they were prepared in air using a Zeiss Stereo Microscope with cross-polarizer for mineralogical separation. For each depth interval, two to five grains were selected on a clean glass slide, both dark (glassy/agglutinate or cubic minerals) and bright under cross-polarized light. Grains were then gently pressed into an indium (99.9975%) foil for XPS and subsequent energy dispersive X-ray analysis (EDAX) in a Phenom XLG2 scanning electron microscope (SEM).

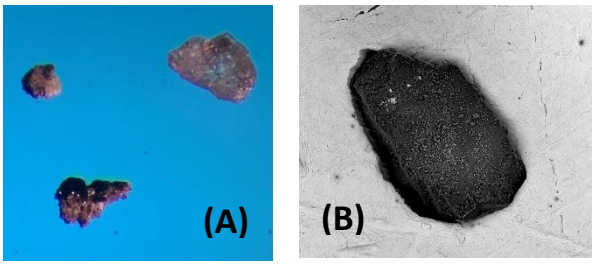

Fig. 1. (A) Reflected-light microscope image of grains from allocation 73002 (249), 1.5-2 cm depth, prior to mounting. (B) SEM image (1050x) of a lunar grain (~150 x 80 µm^2) from allocation 73002 (265), 2.5-3 cm depth, in indium foil without adhesive for XPS analysis.

XPS is a non-destructive near-surface (< 10 nm) analytical technique based on the photoelectric effect that provides quantitative elemental composition, as well as chemical-bond/oxidation state characterization, for species with Z > 2. We used a PHI Versaprobe III XPS microprobe (~6 x 10^{-8} Pa) with a monochromatic X-ray source ($Al_{K\alpha}$: 1486.6 eV) and hemispherical electron energy analyzer to collect survey spectra (1400–0 eV; 0.5 eV/step; ΔE = 2.7 eV) for species identification and high-resolution spectra (0.2 eV/step; ΔE = 0.25 eV) to understand Fe-oxidation surface chemistry. An X-ray beam spot (20 or 50 µm) appropriate to the individual grain size was used, as determined by secondary electron (SXI) imaging, and data was acquired at room temperature. Charge neutralization from an electron flood-gun was utilized during analysis to eliminate variation or change in surface potential during analysis. Data was processed using PHI Multipak, with binding energy scales calibrated to the C-1s peak at 284.8 eV.

Results and Discussion: XPS measured surface composition of grainswithin each interval, regardless of

parent mineralogy, were similar and found to contain: O, Si, Al, Mg, Ca, Fe, Na, C, and F, with many grains also retaining Ti, K, and S throughout the entire 73002 core (Fig. 1). Identified species are similar to elemental bulk compositions as measured by EDAX, which additionally noted Cr, Mn, and Mo in low concentrations in some particles; F was not noted in the bulk analysis. Subsequent XPS analysis of grains (73002, 257) after *in situ* sputtering by 1 keV H removes much of the F, which appears to be ≤ 1 mono-layer, and may be the result of sample collisions with the PTFE-capped containers during transport.

Preliminary XPS data (Fig. 2) describe trends in elemental surface (< 10 nm) concentrations with stratigraphy using average composition of all grains within each 5 mm interval. We find that volatile species (Na, K, S) and Ca are depleted in the surface segments relative to their concentrations deeper in the core, while Fe and Ti are conversely enriched in the near-surface intervals. Si and O content appear relatively constant throughout the 73002 core.

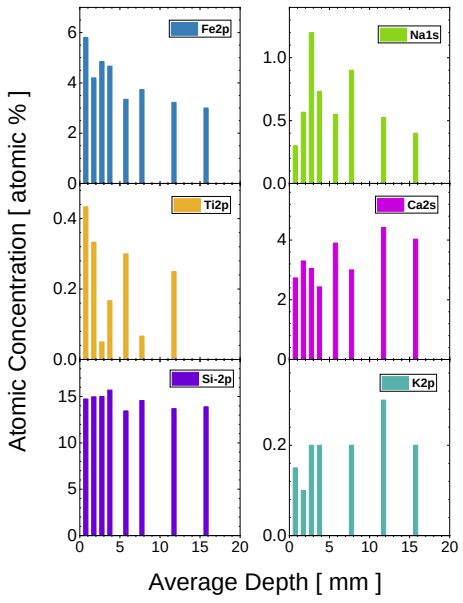

Fig. 2. XPS surface (< 10 nm) elemental composition for 73002 lunar grains from a distribution of depths suggests enrichment in the grain rims of Fe and Ti and near-surface depletion of Na, Ca, and K with distance from the lunar surface.

The Fe-content for grain surfaces can be separated into three general regions within the 73002 core: ≤ 10 mm (5.8 at-%); 15 - 40 mm (4.2 - 4.9 at-%); and ≥ 55 mm (3.0 - 3.7 at-%). Oxidation state information for the iron can be derived from the HR XPS spectra (Fig. 3), and data suggest an enhancement in metallic-component relative to the native (typically Fe^{2+}) chemistry for grains that lie close to the core surface. This result is consistent with measurements of I_s/FeO maturity index, which decrease with depth, identifying mature material within the topmost 30 mm and immature soil for intervals

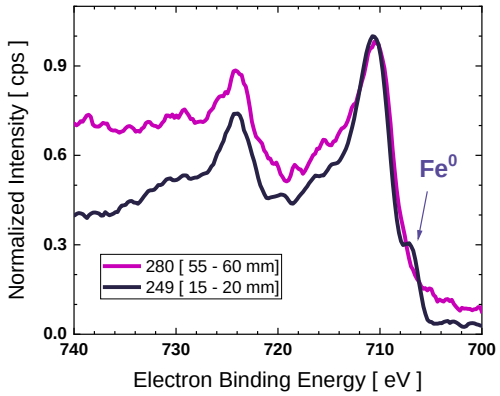

Fig. 3. Comparison of XPS Fe-2p photoelectron feature from near-surface grains (249; 15-20 mm) and from deeper (280; 55-60 mm) into the core show subtle differences in oxidation state suggestive of a metallic Fe component closer to the surface. XPS intensity has been normalized to unity in this region for ease in comparison between spectra with no background removal; BE scale has been shifted for C-1s at 284.8 eV.

below ~ 70 mm [4]. Vis-NIR reflectance measurements for both dissection Pass 1 and Pass 2 find significant darkening (~ 0.22) in the near surface regions (< 30 mm) at 750 nm, relative to material from depth > 10 mm (reflectance ~0.36) [4, 5]. While brightening with depth can signal possible variation in interval mineralogy, it may also suggest the presence of opaque mineral phases, such as nFe^0, which can reduce overall material reflectance [8]. The potential presence of nFe^0 would be indicative of enhanced weathering for the 73002 near-surface intervals, with detailed studies ongoing.

References. [1] Shearer *et al.*, 2020, *LPSC51*, abs1181; [2] Koorotev and Kremser, LPSC22, 275-301; [3] Shearer *et al.*, 2022, *LPSC53*, this conference. [4] Keller and McKay, 1997, GCA 61, 11, 2331-2341 [5] Morris et al., 2022, *LPSC53*, this conference; [6] Sun *et al.*, 2021, *M&PS*, *56*, 1574. [7] Mcfadden *et al.*, 2022, *LPSC53*, this conference. [8] Pieters & Noble, (2016). JGR Planets, 121(10), 1865–1884.